Genome sequence of *Pseudomonas aeruginosa* PAO1161, a PAO1 derivative with the ICEFP2 integrative and conjugative element.

Adam Kawalek[1]*, Karolina Kotecka[1], Magdalena Modrzejewska[1], Grazyna Jagura-Burdzy[1], Aneta Agnieszka Bartosik[1]*

[1] Institute of Biochemistry and Biophysics, Polish Academy of Sciences, Department of Microbial Biochemistry, Warsaw, Poland

* To whom correspondence should be addressed: anetab2@ibb.waw.pl or a.kawalek@ibb.waw.pl.

ABSTRACT

Pseudomonas aeruginosa is a common cause of nosocomial infections, especially in patients with cystic fibrosis and burn wounds. An attenuated PAO1 strain and its derivatives are widely used to study the biology of this bacterium, however recent studies indicated an ongoing evolution of the laboratory strains, highlighted by changes in the genomes of PAO1 sublines and derivatives used in different laboratories worldwide.

Here we have sequenced the genome of *Pseudomonas aeruginosa* PAO1161 strain, a *leu*-, Rif^R, restriction-modification defective PAO1 derivative. This strain is described as the host of IncP-8 plasmid FP2, conferring the resistance to mercury and used in the past for preparation of genetic map of the *P. aeruginosa* chromosome. Comparison of PAO1161 genome sequence with PAO1-UW reference genome revealed an inversion of the large genome segment between *rrnA* and *rrnB* rRNA operons and more than 100 nucleotide polymorphisms and short insertions-deletions, many of which were also found within the recently re-sequenced PAO1 sublines. The PAO1161 specific sequence variants include E108K mutation in PA3792 (*leuA*), which we showed is responsible for leucine auxotrophy, H531L in PA4270 (*rpoB*), likely conferring rifampicin resistance, as well as nonsense mutations in PA2735 encoding a DNA methyltransferase as well as a putative OLD family endonuclease PA1939. Additionally, PAO1161 genome poses a 12 kb RPG42 prophage and a 108 kbp insertion within tRNA-Lys, encompassing a putative mercury resistance and showing similarity to PAPI-1 like integrative conjugative elements (ICE). Our data indicate that the ICE can excise from the bacterial chromosome and can be transferred to *Pseudomonas putida* cells where it integrates in the genome at three specific sites and confers the cells with mercury resistance. Overall this data provide insight into the genome variation between *P. aeruginosa* laboratory strains. Moreover, this data indicate that the FP2 element for years described as a IncP-8 plasmid is an integrative conjugative element.

INTRODUCTION

Pseudomonas aeruginosa is a Gram-negative gammaproteobacterium commonly found in various ecological niches and characterized by the ability to survive in very unfavourable, frequently changing environmental conditions. Being a human opportunistic pathogen, it is often the cause of nosocomial infections in immuno-compromised patients. In cystic fibrosis patients *P. aeruginosa* chronically colonizes the lungs and is a major factor causing mortality (Klockgether and Tümmler, 2017; Azam and Khan, 2018).

Majority of research on this metabolically versatile bacterium uses sublines or derivatives of *P. aeruginosa* PAO1 strain, originally isolated in prof. Bruce Holloway laboratory from a wound of a patient in Melbourne, Australia (Holloway, 1955) Over the years, the strain was shipped to laboratories worldwide and different derivatives, including auxotrophic strains and strains with mobile genetic elements were obtained (Stanisich and Holloway, 1969). In 1999 the genome of *P. aeruginosa* PAO1 stored at the University of Washington (PAO1-UW) was sequenced (Stover et al., 2000), providing a reference for studies on *P. aeruginosa* genomes. As of November 2018, the Pseudomonas Genome Database, a database devoted to the information on *Pseudomonas* species (Winsor et al., 2016), contained 2226 sequenced *P. aeruginosa* genomes, including 11 PAO1 derivatives (sublines). Remarkably, sequencing of PAO1 subline (MPAO1) as well as PAO1-DSM strain stored at the German Collection for Microorganisms and Cell Cultures (DSMZ) revealed presence of multiple short sequence variants which could lead to the variations in virulence and fitness between strains used in different laboratories (Klockgether et al., 2010). A major feature differing genomes of PAO1 derivatives is the occurrence of a large inversion resulting from a homologous recombination between two rRNA operons *rrnA* and *rrnB* (Stover et al., 2000), which is present in the reference PAO1-UW genome and not in MPAO1 and PAO1-DSM (Klockgether et al., 2010). Recent data indicate that, despite displacing the *dif* region, this inversion does not seem to affect chromosome segregation and such large rearrangements could be common among bacteria (Bhowmik et al., 2018). This data indicate an ongoing micro- and macro- evolution of bacterial

genomes and suggests that sequence diversification in laboratory strains should be taken into consideration in the analysis of phenotypic data (Sidorenko et al., 2017; Luong et al., 2014).

In this work we focus on the genome of *P. aeruginosa* PAO1161 strain, a PAO1 derivative requiring leucine for growth on minimal media and selected as lacking the restriction-modification system (*rmo*-10 mutation) (Dunn and Holloway, 1971). This strain is described as the host of IncP-8 plasmid FP2, the only known member of this incompatibility group, conferring bacteria with the resistance to mercury (Finger and Krishnapillai, 1980; Shintani et al., 2015). The FP2 factor has chromosome-mobilizing ability (Cma) and was extensively used in interrupted mating technique for preparation of the genetic map of *P. aeruginosa* chromosome (Stanisich and Holloway, 1969; Holloway and Fargie, 1960).

PAO1161 derives from the PAO38 *leu-38* mutant obtained by treatment of PAO1 with manganus chloride and selection for leucine auxotrophy (Holloway, 1955) (Figure 1A). PAO38 acquired the FP2 element from PAT (*P. aeruginosa* strain 2) (Stanisich and Holloway, 1972) to yield strain PAO170 (Kung and Lee, 1975). Finally, PAO1161 was selected as defective in both restriction and modification systems, called previously host-controlled modification (HCM), following mutagenesis of PAO170 with N-methyl-N'-nitro-N-nitrosoguanidine and a selection, based on the altered susceptibility to phage infection (Rolfe and Holloway, 1968; Dunn and Holloway, 1971). To facilitate genetic manipulations in this strain, *eg*. pAKE600 based allele exchange (El-Sayed et al., 2001), a spontaneus PAO1161 rifampicin resistant clone was obtained (Lasocki et al., 2007). The PAO1161 strain is used in our studies of chromosome segregation and gene expression in *P. aeruginosa* using genome wide approaches (Kawalek et al., 2018; Bartosik et al., 2014; Kawalek et al., 2017) but it is also used in other physiological and genetic studies (Ciok et al. 2018; Komatsu et al., 1994; Manavathi et al., 2005; Kujawa et al., 2017; Papagiannitsis et al., 2013; Laudy et al., 2015; Romaniuk et al., 2017).

Here we report the genome sequence of *P. aeruginosa* PAO1161 strain. Comparison with PAO1-UW reference sequence revealed the presence of a large number of single-nucleotide polymorphisms (SNPs), insertions-deletions (indels), as well as inversion of large genome segment between rRNA genes. Moreover a functional PAPI-1 like integrative conjugative element (ICE), containing a mercury resistance operon was identified in PAO1161 genome, indicating that the FP2 factor is not a plasmid but an ICE named ICEFP2.

RESULTS AND DISCUSSION

Pseudomonas aeruginosa PAO1161 genome was sequenced and assembled, resulting in a single circular chromosome of 6383803 bp. The GC content (66.42 %) was similar to those of other *P. aeruginosa* genomes (Mathee et al., 2008). A comparison with the reference PAO1-UW genome (NC_002516) revealed three major structural differences (Figure 1B). PAO1161 genome lacks the large inversion between ribosomal RNA operons *rrnA* and *rrnB* observed in PAO1-UW but not in other PAO1 derivatives including MPAO1 and PAO1-DSM (Klockgether et al., 2010). Additionally, PAO1161 poses two large insertions. The 107796 bp insertion in tRNA-Lys gene between *lepA* (*PA4541*) and *clpB* (*PA4542*), flanked by 48 bp repeated sequences, displays a significant similarity to PAPI-1 like integrative conjugative elements (discussed below) (Liu et al., 2018; Qiu et al., 2006). The second 11981 bp insertion between tRNA-Met (*PA4673.1*) and *higA* (*PA4674*), flanked by 82 repeated bp, is identical to the prophage-like RGP42 element identified in MPAO1 and PAO1-DSM (Klockgether et al., 2010). Additionally, PAO1161 lacks a 280 bp fragment containing PA1796.3 and PA1796.4 tRNA genes and has an 107 bp insertion downstream of PA2327.

Impact of PAO1161 / PAO1-UW sequence variation on gene structure

A comparisons of PAO1161 and PAO1-UW genome sequences using Nucdiff (Khelik et al., 2017) revealed 251 single nucleotide polymorphisms (SNPs), multiple nucleotide polymorphisms (MNPs) and short insertions / deletions (indels). Since a direct sequence comparison does not provide information about quality of predicted variants the outcome can be greatly affected by errors during genome sequence consensus calling, caused for instance by mapping of reads derived from highly similar sequences to another, very similar, parts of the genome. To identify high quality variants we aligned the reads used in genome assembly to the consensus sequence and checked the coverage of the region with reads, their mapping quality as well as frequency of the variant at a given genome position. The variants present in more than 80% of the reads were considered as homozygous. Overall 100 SNPs/MNPs/indels were called with a high confidence between the PAO1161 and the PAO1-UW reference. The remaining (heterozygous) variants were mostly SNPs

(149/151) located in coding sequences of genes belonging to Pseudomonas Orthologous Groups (POG) possessing multiple same strain members (multiple orthologs within PAO1 genome) (Winsor et al., 2016). This group included 17 SNPs in PA0723-PA0726 genes from the Pf1 cryptic prophage region syntenic to the genes within RGP42 element also present in PAO1161 genome (Klockgether et al., 2010). Eight of these variants were also identified previously in MPAO1 and PAO1-DSM (Klockgether et al., 2010), nevertheless these did not meet our quality criteria.

The high-confidence variants encompassed 52 SNPs, 6 MNPs, 15 deletions and 27 insertions. Of these 44 were mapping to intergenic regions in PAO1-UW genome and 9 were synonymous (silent) mutations (Supplementary Table S1). Five identified variants lead to frame shifts, resulting in expression of truncated proteins (Table 1). Three of these mapped to the 3' part of the genes, resulting in short sequence alterations, unlikely to affect the function of corresponding protein products (Table 1). Moreover similar shorter versions of the encoded proteins were found for other representatives of related POG (POG001263, POG003705, POG003333, respectively) indicating that such shortened version of PA1327, PA1685 or PA2141 homologues are more frequent among *Pseudomonas* species. Relative to PAO1, PAO1161 genome contains a frame shift in the PA0683 (*hxcY*) gene encoding a component of the Hxc system, a type II secretion system active under phosphate-limiting growth conditions and dedicated to the secretion of low-molecular-weight alkaline phosphatases LapA and LapB (Cianciotto and White, 2017; Ball et al., 2002, 2012).

Two more mutations resulted in an introduction of premature stop codons (Table 1). These are in PA2735 gene, recently shown to encode a N6-adenosine DNA methyltransferase acting on a conserved sequence (Doberenz et al., 2017), and in PA1939, encoding a putative overcoming lysogenization defect (OLD) family nuclease containing an N-terminal ATPase domain and a C-terminal TOPRIM domain (Aravind et al., 1998). Since *P. aeruginosa* PAO1161 strain was selected as defective in its restriction system (Dunn and Holloway, 1971; Rolfe and Holloway, 1968), it is tempting to speculate that PA1939 could be the protein involved in degradation of foreign DNA.

Together with PA2735 this protein could constitute the chromosomal restriction-modification system of *P. aeruginosa*.

In contrast, 14/15 of the identified sequence variants could lead to an extension of the predicted protein product (Table 2). These include 413850 T→C mutation upstream of PA0369, removing an in frame stop-codon and possibly leading to a translation of a longer protein. Similar, start codon changing role can be attributed to nucleotide differences/changes within PA2046-PA2047 and PA4874-PA4875 intergenic regions, as well as to 5 other indels (Table 2). The effect of three sequence variants was a fusion of proteins encoded by neighbouring genes in PAO1-UW genome into one protein in PAO1161. Additionally, the frameshift observed in PAO1-UW in PA0748 gene, encoding an AraC type transcriptional regulator, is not observed in PAO1161. Notably, analysis of the sequences composing Pseudomonas Orthologs Groups (www.pseudomonas.com) of corresponding PAO1 genes showed that the modified (PAO1161-like) protein products constitute a vast majority of all sequences (in comparison to PAO1 reference like sequences), indicating that for these genes PAO1-UW reference may not represent protein products of other strains and *Pseudomonas* species.

Effect of SNPs, MNPs and indels

Except sequence variants affecting the gene structure, numerous SNPs and indels resulting in amino acid changes relative to corresponding PAO1-UW genes/proteins were identified in PAO1161 genome (Table 3). One special case is PA2492 (*mexT*), where both a deletion and a SNP were observed in PAO1161 relative to PAO1-UW genome (Table 1, 3). MexT is a LysR type transcriptional regulator activating expression of the MexEF-OprN multidrug efflux system, extensively studied in the context of quorum sensing signalling and resistance to antimicrobial agents (Köhler et al., 1999; Uwate et al., 2013; Köhler et al., 2001; Lamarche and Déziel, 2011). PAO1161 does not possesses the 8-nt insertion within *mexT* (Table 1), observed in some PAO1 sublines (Maseda et al., 2000). Concomitantly, PAO1161 contains a SNP in the *mexT* gene, leading to F172I change which is also found in most of the strains lacking the 8-nt insertion in *mexT*

(Maseda et al., 2000). A sequence variation was also observed in *mexS*, encoding a negative regulator of MexT (Uwate et al., 2013; Sobel et al., 2005; Fargier et al., 2012), resulting in D249N amino acid change. Recent data indicate that the MexS protein with this amino acid change appears to be fully functional (Uwate et al., 2013). The presence of functional *mexT*/*mexS* system in PAO1161 is strengthened by the observation that this strain shows low resistance to chloramphenicol (MIC < 64 µg/ml), whereas the *mexT* defective PAO1 sublines are extremely resistant to this antimicrobial (Luong et al., 2014; Maseda et al., 2000).

PAO1161 strain derives from the strain PAO38 which was selected as the leucine auxotroph (Figure 1A). Genome sequencing of PAO1161 revealed that this strain possess E108K mutation in PA3792 (*leuA*), encoding a putative 2-isopropylmalate synthase. Analysis of Pseudomoans Orthologue Group of the *leuA* (POG001874) showed that, the only other *P. aeruginosa* strains carrying this mutation are PAO579 (Ryan Withers et al., 2013) and PAO581 (Yin et al., 2013), both derived from PAO38. To validate that this mutation is responsible for/causing the leucine auxotrophy, we reversed the mutation. The exchange of the mutant allele by PAO1 gene fully restored the ability of PAO1161 strain to grow on minimal medium without leucine (Figure 2AB), confirming that the E108K mutation in PA3792 (*leuA*) caused leucine auxotrophy.

P. aeruginosa PAO1161 used in our study was a spontaneous rifampicin resistant clone (Lasocki et al., 2007). Rifampicin acts by binding to a conserved pocket on the β-subunit of RNA polymerase therefore blocking RNA transcript elongation (Campbell et al., 2001). Resistance to this drug results from mutations on the *rpoB* gene that change the structure of the pocket (Campbell et al., 2001; Severinov et al., 1993; Hall et al., 2011). Our SNP analysis revealed presence of H531L mutation in PA4270 (*rpoB*) encoding *P. aeruginosa* DNA-directed RNA polymerase subunit beta (Table 3). The *rpoB* H531L mutation was frequently observed in spontaneous *P. aeruginosa* Rif^r mutants (Jatsenko et al., 2010), strongly indicating that this SNP confers PAO1161 strain with rifampicin resistance.

From 26 SNPs and indels identified in PAO1161 resulting in amino acid changes relative to corresponding PAO1-UW proteins, 15 seem to be strain (PAO1161) specific (Table 3, bolded gene names). Examples include codons deletion identified in PAO1161 genes encoding a pimeloyl-CoA synthetase PauA (PA1017) involved in biotin synthesis (Binieda A et al., 1999), a transcriptional regulator PA3067 from MarR family or a sensor histidine kinase KinB. The KinB as a part of two-component system is involved in phosphorylation/dephosphorylation of the transcriptional regulator AlgB and control of alginate and virulence factors production in *P. aeruginosa* (Ma S. et al., 1997; Damron et al., 2009; Chand et al., 2012; Balasubramanian D et al. 2013). The point mutation changing amino acid sequence R221H was also detected in PAO1161 *algB* (Table 3).

A start codon shift in *relA* gene encoding a GTP pyrophosphokinase in PAO1161 relative to PAO1-UW was identified (Table 3). It raised the question, if this protein is expressed in PAO1161. Performed sequence analysis showed a possibility of translation starting from a valine codon generated at the beginning of the changed *relA* in PAO1161. Indeed, proteomic analysis of PAO1161 strain using mass spectrometry and iTRAQ quantification demonstrated that the RelA is produced in PAO1161 (Malinowska A. et al. 2012). This protein together with SpoT plays an important role in controlling the level of the alarmone guanosine 5'-triphosphate-3'-diphosphate (ppGpp) involved in bacterial adaptive responses and virulence (Xu X Yu H et al., 2016),

Among identified indels comparing predicted gene products of PAO1161 and PAO1 the codon insertion change in PA5024 locus encoding conserved hypothetical protein with transmembrane domain was identified. Deeper analysis of homologues of this protein from POG004631 showed that the modified shortened version of PA5024 are characteristic only for few close relatives of PAO1 (e.g. PAO579, PAO581, PAO1-VE2), while the vast majority of sequences represents the longer version of the protein similar to that of PA5024 from PAO1161.

Several PAO1161 specific mutations corresponding to a single amino acid changes were also identified (Table 3). Examples include aa substitutions in proteins involved in different metabolic processes e.g. the change T103I in the transcriptional regulator GcdR engaged in

regulation of glutarate utilization and lysine catabolism (Indurthi et al., 2016), A232T in the carbamate kinase ArcC involved in fermentative arginine degradation (Schreiber et al., 2006), V126M in the ribonuclease E (*rne*) involved in mRNA turnover (Kushner, 2004). The G108D change was identified in Tsi4 of PAO1161 relative to corresponding protein of PAO1. This protein is a part of antibacterial effector-immunity pair together with type VI secretion exported toxin Tse4 (PA2774) (Whitney et al., 2014). These could influence the structure and/or function of the corresponding protein and therfore care should be taken in analyses of these genes using PAO1161 strain.

PAO1161 genome contains an ICE conferring resistance to mercury

PAO1161 was described as a strain containing the IncP-8 plasmid FP2, which confers the cells with mercury resistance. Indeed, the strain used in our lab was exceptionally resistant to mercury, showing growth in LB medium with up to 200 μM $HgCl_2$ (Ciok et al., 2018) (and data not shown), confirming presence of the element. Surprisingly, during genome assembly no extra-chromosomal elements could be identified. Instead, an almost 108 kbp insertion in the chromosome, with a putative mercury resistance operon, was found (Figure 1B, Figure 3A). The insertion shows similarities (in sequence and organization of operons flanking the putative integration site) to the PAPI-1 family of integrative conjugative elements (ICE) (Liu et al, 2018; Qiu et al., 2006; Johnson and Grossman, 2015). ICEs are mobile genetic elements, with modular structure, encoding complete conjugation machinery (usually a type IV secretion system) allowing transfer of their genome to another host. They are reversibly integrated into a host genome and can be passively propagated during bacterial chromosome segregation and cell division (Johnson and Grossman, 2015; Delavat et al., 2017; Wozniak and Waldor, 2010). PAPI-1 was first described in the genome of highly virulent *P. aeruginosa* PA14 strain (He et al., 2004). It has a size of 108 kbp, encodes 115 predicted genes, integrates into $tRNA_{Lys}$ gene and represents an abundant family of ICEs with a similar gene structure, present in *Pseudomonas* genomes (Liu et al., 2018). Integrated PAPI-1-like ICEs contain an operon starting with a gene encoding an orphan F-type ATPase, with high

similarity to Soj/ParA proteins involved in segregation of chromosomes and plasmids, adjacent to the integration site (Qiu et al., 2006). At the other end of the integrated ICE, an operon encoding a putative relaxase (*traI*) and a tyrosine type site specific recombinase is encoded. The element identified within PAO1161 genome has an integration site within a tRNALys and PAPI-1 like organization of boundary operons (Figure 3A). According to the ICEberg database, this family encompasses PAPI-1(He et al., 2004), PAGI-5 (Battle et al., 2008), PFGI-1 (Mavrodi et al., 2009), pKLC102 (Klockgether et al., 2004), ICE*Pae*2192-1, ICE*Pae*C3719-1 and ICE*Pae*PACS2-1(Liu et al., 2018). Analysis of gene content (Supplementary Table S2), revealed that out of 120 predicted genes within the putative ICE, 102 genes are found in at least of the 5 other PAPI-1 like elements, whereas orthologs of 41 genes are found in all ICE analysed (Supplementary Table S2). These data indicate high similarity of the putative ICE identified in PAO1161 genome with PAPI-1 like elements.

Integration of ICE into the chromosome as well as its excision is mediated by a an ICE encoded site directed recombinase / integrase (Grindley et al., 2006). Recombination between a attachment site in the chromosome (*attB*) and the corresponding site on an circular ICE (*attP*) leads to integration of the element in the genome, now flanked by identical *attL* and *attR* sequences (Figure 3B). Excision of the putative ICE from the PAO1161 chromosome, as well as presence of a stable circular form was analysed using PCR with primers flanking the *att* sequences (Figure 3BC). The analysis confirmed presence of the circular ICE in PAO1161 cells (Figure 3C), indicating that the element can be excised from the chromosome.

To verify that the ICE can be transferred to another host, we inserted a streptomycin resistance cassette within the ICE. Subsequently, PAO1161::ICE-Sm^R strain was used as an ICE donor for mating in static liquid cultures with *Pseudomonas putida* KT2440 as a recipient. Conjugants were selected on M9 plates supplemented with streptomycin, but lacking leucine to block the growth of donor cells. Streptomycin resistant *P. putida* clones were obtained at an efficiency of $2x10^{-7}$ conjugants / donor cell.

To confirm that the *P. putida* conjugants show also enhanced resistance to mercury, attributed to the presence of *mer* operon within the ICE, we analysed the growth of conjugants in medium containing $HgCl_2$. The recipient *P. putida* KT2440 cells were unable to grow at a $HgCl_2$ concentration higher than 2 μM (Figure 3D and data not shown). In contrast, the growth of streptomycin resistant *P. putida* conjugants was not inhibited by addition of 40 μM $HgCl_2$ to the medium, confirming acquisition of mercury resistance (Figure 3D).

Finally, to confirm that the ICE, transferred from PAO1161, integrated in *P. putida* KT2440 chromosome we searched for putative *attB* sites in the genome using the 48 bp TGGTGGGTCGTGTAGGATTCGAACCTACGACCAATTGGTTAAAAGCCA sequence flanking the ICE in PAO1161 chromosome. *P. putida* KT2440 genome contains three potential attachment sites called *attB1-3*, with the *attB1* and *attB2* located adjacent to each other (Figure 3E). A PCR analysis, using primer pairs specific to the ICE/chromosome junctions revealed a highly oriented integration of the putative ICE in the genome (Figure 3F). In individual clones, the specific PCR product was observed for one or more of the 3 attachment sites (Figure 3F). The orientation of the ICE in chromosome was determined by the orientation of the *att* site (Figure 3EF, blue arrows), as the PCR analysis only confirmed integration in an orientation resembling the one observed in PAO1161 genome (Figure 3C and data not shown). Overall, these data confirm the ability of the ICE identified in the PAO1161 genome to transfer to another host.

Conclusions

In this work we show that *P. aeruginosa* PAO1161 strain carries a PAPI-1 family integrative conjugative element capable of excision, transfer and integration in the genome of a closely related strain. The ICE contains an operon conferring mercury resistance, in the past attributed to the FP2 plasmid, the only member of IncP-8 incompatibility group. Our data indicate that FP2 is an integrative conjugative element and we propose to rename this element to ICEFP2.

The genomic features of *P. aeruginosa* PAO1161, a close derivative of reference PAO1 strain, were identified based on the complete genome sequence. Our data indicate a number of

sequence variants, likely affecting different aspects of cell physiology. Thus genome sequencing of laboratory strains is highly recommended to provide full information of genotype and help in interpretation of observed phenotypes under the conditions studied.

MATERIALS AND METHODS

Bacterial strains and growth conditions

P. aeruginosa strains used were PAO1161 (*leu*$^-$, *r*$^-$, *m*$^+$), kindly provided by B. M. Holloway (Monash University, Clayton, Victoria, Australia) and its derivative PAO1161 Rif^R (Lasocki et al., 2007), PAO1161 Rif^R ICERP2^Sm^R (this work). *Escherichia coli* strain DH5α [F$^-$(*ϕ80*d*lac*ZΔM15) *recA1 endA1 gyrA96 thi-1 hsdR17*($r^-_K m^-_K$) *supE44 relA1 deoR* Δ(*lacZYA-argF*)*U196*] was used for all plasmid constructions and S17-1 (*pro hsdR hsdM recA* Tp^R Sm^R ΩRP4-Tc : :Mu-Km : : Tn7) (Simon et al., 1986) was used to mate plasmids into *P. aeruginosa*. Details of plasmid and strain constructions are provided in Supplementary Material.

Bacteria were grown in Luria broth (Kahn et al., 1979) at 37°C or on Luria agar (Luria broth with 1.5% w/v agar) supplemented with antibiotics as appropriate: benzylpenicillin sodium salt at 150 μg ml^{-1} in liquid medium and 300 μg ml^{-1} on agar plates for penicillin resistance in *E. coli*, streptomycin at 30 μg ml^{-1} for streptomycin resistance in *E. coli*, streptomycin at 150 μg ml^{-1} for streptomycin resistance in *P. aeruginosa* and *P. putida*, carbenicillin at 300 μg ml^{-1} for carbenicillin resistance in *P. aeruginosa*, rifampicin at 300 μg ml^{-1} for rifampicin resistance in P. *aeruginosa*. Some experiments were performed in M9 minimal medium (Sambrook et al., 1989) supplemented when indicated with leucine (10 μg ml^{-1}) or glucose (0.1%).

Bacterial growth was monitored by measurements of optical density at 600 nm (OD_{600}) using spectrophotometer UV1000 (Shimadzu) or Varioskan Lux Multimode Microplate Reader with SkanIt RE 5.0 software (Thermo Fisher Scientific).

Plasmids, oligonucleotides and DNA manipulations

The plasmids used and constructed during this study as well as primers are listed in Supplementary Table S1. Plasmid DNA was isolated by alkaline method and standard genetic procedures were used as recommended (Sambrook et al., 1989). Chromosomal DNA templates for PCRs were prepared from 100 µl overnight cultures of appropriate strains. Pelleted cells were washed with sterile water, re-suspended in 100 µl of sterile ddH_20, boiled and centrifuged 10 min at 4^oC at maximum speed. Standard PCR was performed using 1 µl of boiled cell suspension as a template, 5 pmoles of each primer and DreamTaq polymerase (Thermo Fisher Scientific) in recommended buffer. Fidelity of the amplified DNA sequence was verified by DNA sequencing in the internal sequencing facility (DNA Sequencing and Oligonucleotides Synthesis Laboratory, IBB PAS, Warsaw, Poland).

PCR site-directed mutagenesis

The QuickChange site-directed mutagenesis method was applied (Stratagene) with the pAKE600 plasmid (El-Sayed et al., 2001) derivatives containing *pa3972* gene and ICE fragment, respectively. The presence of change/mutation was verified by DNA sequencing of PCR-amplified fragments.

Bacterial transformation

Competent *E. coli* cells were prepared by the standard $CaCl_2$ method (Sambrook et al., 1989).

Introduction of *pa3972* and ICE::*addA* [$Sm^{R]}$ fragment into *P. aeruginosa* PAO1161 chromosome by homologous recombination

The competent *E. coli* S17-1 cells were transformed with pAKE600 suicide vector derivatives to construct donor strains for conjugation. Bacterial conjugation was done on L-agar by mixing 100 µl of overnight cultures of *E. coli* S-17 (pAKE600 derivatives) donors and *P. aeruginosa* PAO1161 [$Rif^{R]}$ recipient strain and incubation for 24 h at 37°C. The bacterial mixtures were washed off the plates with 2 ml of L-broth, and diluted cell suspensions were plated on L-agar with rifampicin and carbenicillin for *pa3972* allele exchange and with rifampicin, carbenicillin and streptomycin for ICE::*addA* [Sm^R] selection of transconjugants/integrants.

The integrants of PAO1161 Rif^R (pAKE600 derivatives) were treated as described previously (Lasocki et al., 2007). The allele integration and then allele exchange was verified by PCR using

chromosomal DNA as a template and the adequate pairs of primers and by confirmation of streptomycin resistance for PAPO1161 ICE::*addA* [Sm^R] derivatives.

ICE transfer to *P. putida*

P. aeruginosa PAO1161- ICE[Sm^R] was used as a donor and *P. putida* KT2442 [Rif^R] was used as the recipient strain in ICE transfer/mobility testing. 1 ml of overnight cultures of the donor and recipient strains in liquid LB were centrifuged (1 min, 6500 rpm), the supernatant was discarded and cells suspended in 1 ml of fresh liquid rich medium. The donor and recipient strains were mixed in Eppendorf tubes in different ratio of donor to recipient (1:2; 1:4; 1:8) adding 100 μl of donor strain and appropriate volume of recipient cells. The mixtures were incubated for 2 h at 37°C with shaking and then 3 h without shaking. Then the mixtures were centrifuged at 6500 rpm for 1 min, the supernatant pour out and the cells suspended in the initial volume of 0.9% NaCl. To estimate the number of transconjugants a serial dilution of bacteria in 0.9% NaCl solution was performed and aliquots of serial 10-fold dilutions were plated onto M9 minimal medium agar plates with 0.1% glucose and 150 μg ml^{-1} streptomycin without leucine. Lack of leucine in plates with M9 medium allows selection of *P. putida* KT2442 transconjugants (*leu*$^+$) and elimination of PAO1161 *leu*$^-$ donor cells since they need supplementation of leucine on minimal media. In parallel 100 μl of donor or recipient strain cultures, respectively were treated the same way to establish the titer of donor and recipient cells in the conjugation mixture. The transfer frequency was calculated as number of transconjugants per donor cell.

Mercury resistance testing of *P. putida* ICE transconjugants

Analytical grade salt HgCl2 was used in a resistance assay performed in 96-well plates employing Varioskan Lux Multimode Microplate Reader with SkanIt RE 5.0 software (Thermo Fisher Scientific). Triplicate cultures of each strain/transconjugant were challenged with a range of concentrations of mercury chloride in liquid rich medium (2-400 μM). The derivatives of *P. putid*a KT2442 that grew in the presence of HgCl2 at concentrations higher that 2 μM were considered resistant.

Genome sequencing and assembly of sequence reads

To unravel the genomic properties of *P. aerugionsa* PAO1161 strain whole genome sequencing (WGS) was carried out. Bacterial total genomic DNA was isolated using CTAB/lysozyme method (Wilson et al., 1987) with addition of cell wall degrading enzyme: lysozyme (20 mg/ml; Sigma-Aldrich, Dorset, UK). DNA quality was checked on standard 0.8% agarose gel, 1% PFGE gel on Biorad CHEF-III apparatus and template quantity was measured using Qubit v3.0 fluorimeter. Genomic bacterial DNA was mechanically sheared to appropriate size and used for Paired-End TruSeq-like libraries construction using KAPA Library preparation kit (KAPA/Roche, Basel, Switzerland) following manufacturer's instructions. The bacterial genome was sequenced in paired-end mode (v3, 600 cycle chemistry kit) using MiSeq instrument (Illumina, San Diego, CA). Illumina sequencing yielded 23 380 926 reads and 4 676 185 200 nucleotides of sequence data. Obtained sequence reads were filtered by quality using FastX toolkit (http://hannonlab.cshl.edu/fastx_toolkit/) and residual Illumina adapters were removed using Cutadapt (https://github.com/marcelm/cutadapt). Quality filtered and subsampled to 700 million nucleotides Illumina data (7 000 000 paired reads) was assembled using Spades v3.11.1 (http://cab.spbu.ru/software/spades/) to estimate approximate size of draft bacterial genome. In the next stage long reads were generated using MinION nanopore sequencing instrument (Oxford Nanopore Technologies, Oxford, UK). Bacterial DNA was sheared into approximately 20 kb fragments using Covaris gTube (Covaris, Ltd., Brighton, United Kingdom) and the library was prepared using the ONT 1D ligation sequencing kit (SQK-LSK108) with the native barcoding expansion kit (EXP-NBD103). Nanopore sequencing was performed using the NC_48□h_Sequencing_Run_FLO-MIN106_SQK-LSK108 protocol, R9.4.1 MinION flowcell and MinION MkIB instrument. Raw nanopore data was basecalled using Albacore v2.3.1 (Oxford Nanopore Technologies, Oxford, UK). After quality filtering and sequencing adapter removal using Porechop (https://github.com/rrwick/Porechop) and NanoFilt (De Coster et al., 2018) 161877 barcoded reads remained. The median read length of obtained dataset was 12489 nucleotides and 2

160 720 766 of total bases. Long nanopore reads were assembled in a hybrid mode with Illumina data using Unicycler v.0.4.6 (Wick et al. 2017). Genome hybrid assembly resulted in 1 circular replicon of the size 6 383 803 bp. The remaining sequence errors in the genome assembly were verified by the PCR amplification of DNA fragments, followed by Sanger sequencing with an ABI3730xl Genetic Analyzer (Life Technologies, USA) using BigDye Terminator Mix v. 3.1 chemistry (Life Technologies, USA). All of the sequence errors and missassemblies were further corrected using Seqman software (DNAStar, USA) to obtain complete nucleotide sequence of bacterial genome.

Genome annotation

The assemblies were mapped against *P. aeruginosa* reference genome POA1 to evaluate the core genome average identities and completeness. The finalized draft genome was submitted to NCBI Prokaryotic Genome Annotation Pipeline (PGAP) server for gene predictions and annotations. Prokka Version 1.11 (Prokaryotic annotation) was used to perform the gene prediction (Seemann, 2014). The prediction was relied on the existing annotation resources such coding DNA sequences (CDS) and proteins.

Analysis of single nucleotide polymorphism (SNP)

To identify genetic differences at genome level, the sequencing reads of PAO1161 strain were mapped to its corresponding reference genome *P. aeruginosa* POA1 using Bowtie v0.12.0 software (Langmead et al., 2009). SNPs and indells between the 2 consensus sequences were called using Nucdiff (Khelik et al., 2017). The effect of SNP was predicted using snpEff (Cingolani et al., 2012).**Genome comparison**

Protein Basic Local Alignment Search Tool (BLASTp) was used to match the sequence similarities between PAO1161 genome and the *P. aeruginosa* reference genome PAO1 (Altschul et al., 1997).

Nucleotide sequence accession numbers. The nucleotide sequence of the PAO1161 described in this paper has been deposited in the GenBank database (accession number CP032126).

SUPPLEMENTARY MATERIALS

Supplementary Material S1. Details of plasmid and strain constructions.

Supplementary Table S1. SNPs identified in PAO1161 genome. Non-synonymous SNP's are bolded.

Supplementary Table S2. Gene content of ICEFP2 from PAO1161.

Supplementary Table S3. Plasmids, primers used in this study.

ACKNOWLEDGEMENTS

This work was funded by National Science Centre, Poland [2015/2015/18/E/NZ2/00675 granted to A.A.B. and in part by 2013/11/B/NZ2/02555 granted to G.J.B.]. DNA sequencing was performed by DNA Sequencing and Oligonucleotides Synthesis Laboratory, IBB PAS, Warsaw, Poland.

Conflict of interest statement. None declared.

FIGURE LEGENDS

Figure 1. (A) How PAO1 became PAO1161? History of PAO1 derivatives. **(B)** Pairwise nucleotide sequence comparison of the *P. aeruginosa* PAO1-UW reference strain and genome sequence of PAO1161. An inversion of the large genome segment between *rrnA* and *rrnB* rRNA operons is demonstrated. Positions and schematic gene organization of identified in PAO1161genome mobile/integrative elements: ICEFP2 and RGP42 are showed.

Figure 2. Growth of PAO1161 *leu*$^{+}$ revertant on minimal medium **(A)** on solid agar and **(B)** in liquid cultures. The PAO1161 *leu*$^{-}$ is showed for comparison including growth on minimal medium with leucine.

Figure 3. Integrative and conjugative element of PAO1161 – ICEFP2. **(A)** Comparison of gene organization of PAO1161 ICEFP2 with other representative integrative and conjugative elements identified in *P. aeruginosa* strains. The boxes with arrows indicate individual ORFs and their transcriptional orientation. ORF colour corresponds to the predicted protein function in each mobile

element. Gene operons/clusters involved in maintenance and regulation functions, conjugation and excision are marked. The coloured regions show the homology between analysed integrative elements. **(B)** Model of ICEFP2 excision from the chromosome. Thin, orange arrows indicate the primers used for detection of integrated and circular ICEFP2 form. The genes are not drawn to scale. **(C)** PCR products obtained with indicated primer pairs detecting the integrated and circular ICEFP2 as well as empty integration site in PAO1161, respectively. **(D)** Growth of *P. putida* KT2440 in rich medium containing 40 µM $HgCl_2$. Growth curves of *P. putida* KT2440 recipient strain and *P. putida* KT2440 carrying ICEFP2 from PAO1161 in L broth and L broth supplemented with $HgCl_2$ at 37°C, respectively. **(E)** Three potential integration sites *attB* (in blue) in *P. putida* KT2440 genome and ICEFP2 integration in one orientation at each *attB* site are schematically showed. **(F)** Detection of ICEFP2 in *P. putida* KT2440 conjugants. Six independently obtained transconjugants was analysed. PCR products obtained with indicated primer pairs detecting the integrated ICEFP2 in *P. putida* KT2440 are presented.

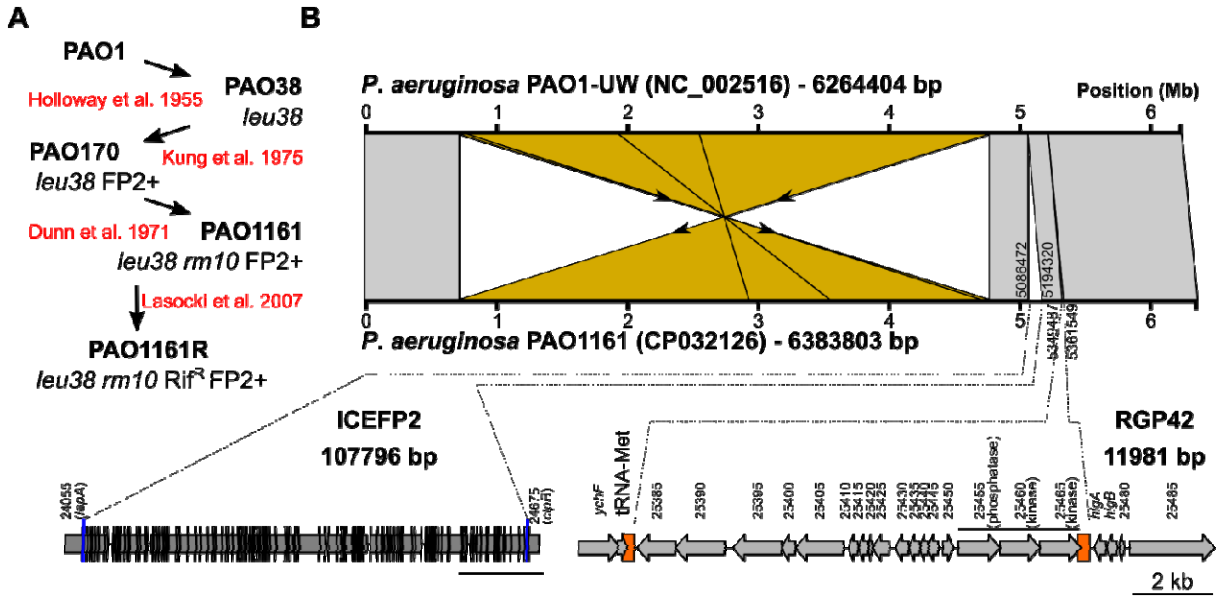

Figure 1

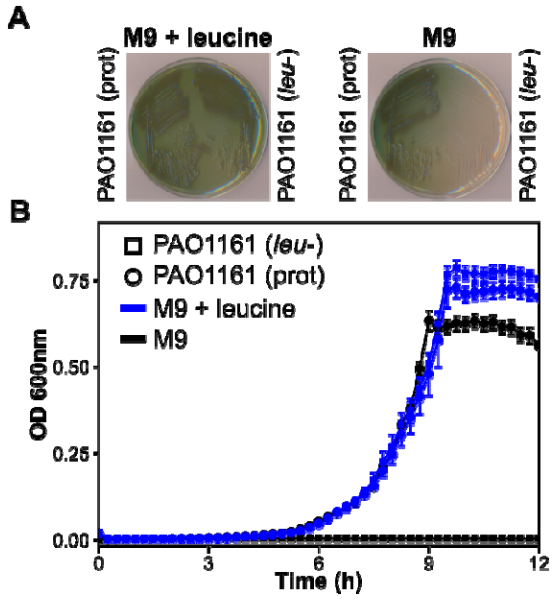

Figure 2

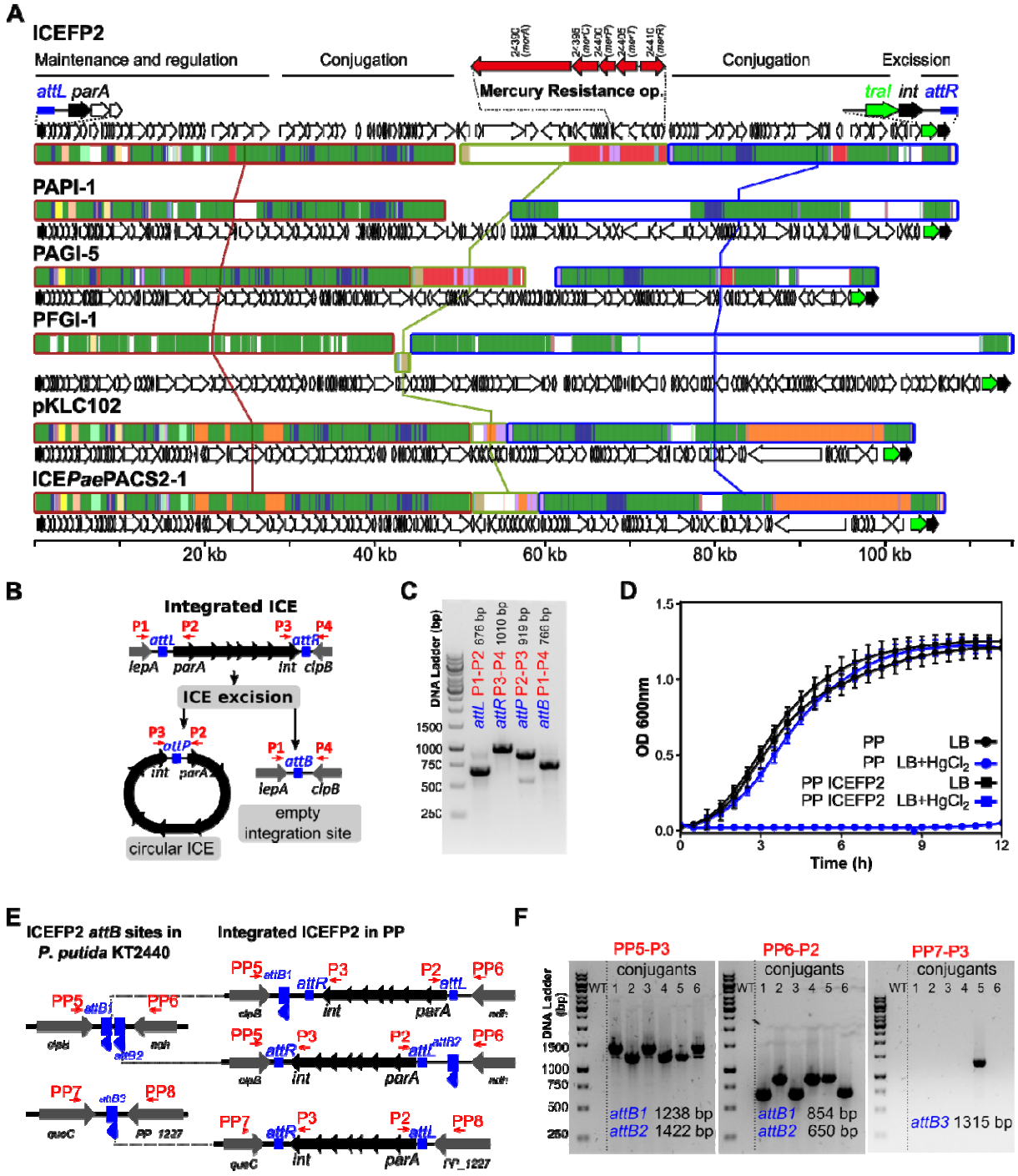
A
ICEFP2
Maintenance and regulation
Conjugation
Mercury Resistance op.
Conjugation
Excission
attL parA
traI int attR
PAPI-1
PAGI-5
PFGI-1
pKLC102
ICEPaePACS2-1
20 kb
40 kb
60 kb
80 kb
100 kb
B
Integrated ICE
P1 P2 P3 P4
attL attR
lepA parA int clpB
ICE excision
P3 P2
attP
int parA
P1 P4
attB
lepA clpB
circular ICE
empty integration site
C
DNA Ladder (bp)
1500
1000
750
500
250
attL P1-P2 676 bp
attR P3-P4 1010 bp
attP P2-P3 919 bp
attB P1-P4 766 bp
D
OD 600nm
Time (h)
PP LB
PP LB+HgCl2
PP ICEFP2 LB
PP ICEFP2 LB+HgCl2
E
ICEFP2 attB sites in P. putida KT2440
Integrated ICEFP2 in PP
PP5 PP6
attB1 attB2
clpB nah
PP7 PP8
attB3
queC PP_1227
P3 P2
attR attL
int parA
F
PP5-P3
PP6-P2
PP7-P3
conjugants
WT 1 2 3 4 5 6
attB1 1238 bp
attB2 1422 bp
attB1 854 bp
attB2 650 bp
attB3 1315 bp

Figure 3

Table 1 SNPs and indels identified in *P. aeruginosa* PAO1161 genome, possibly resulting in expression of truncated proteins.

Mutationeffect	PAO1-UW position	Nucleotide change	AA change	length PAO1/ PAO1161	PAO1 gene	PAO1161 ID	Description
stop gained	2121203	C → T	W340*	665 /339	PA1939	D3C65_15950	Probable ATP-dependent endonuclease of the OLD family
	3097884	G → A	Q209*	792 / 208	PA2735	D3C65_11725	SAM-dependent DNA methyltransferase
frame-shift	740419	G → GC	V73A?	381 / 124	PA0683 (*hxcY*)	D3C65_22610	probable type II secretion system protein
	1440623	AA → A	K640	656 /642	PA1327	D3C65_19175	probable protease
	1835045	G → GC[†]	S218S?	249 / 226	PA1685 (*masA*)	D3C65_17305	enolase-phosphatase E-1
	2356682	CC → C	L173	182 /172	PA2141	D3C65_14865	CinA family protein
	2807706	CAGCCGGCC → C	aa1-78/ 35aa	347 / 304	PA2492 (*mexT*)	D3C65_13040	transcriptional regulator MexT

[†] - SNP at this position in PAO1DSM / MPAO-1 (Klockgether et al., 2010) but a nucleotide insertion in our study

Table 2 SNPs and indels identified in *P. aeruginosa* PAO1161 genome influencing the reading frames of genes and possibly leading to longer protein products. The effect of a mutation is predicted using the PAO1-UW genome as a reference. The possibility of the production of a longer protein was validated by comparison of the predicted sequence with sequences from corresponding Pseudomonas Ortholog Group (POG) at pseudomonas.com.

Position in PAO1-UW	Nucleotide change	PAO1 loci	PAO1161 loci	Effect of mutation
413850	T → C	IG: PA0369-PA0370	D3C65_01955	TGA codon -12 to -10 of PA0369 start codon is removed. Longer (30 aa) PA0369 can be translated. Similar extension observed for 297/303 members of POG000360.
816531	C → CC	PA0748	D3C65_22250	Corrects the reading frame of PA0748 (still frameshift orf).
1116213	G → GC	PA1029	D3C65_20745	Removes start codon of PA1029. Predicted product has additional 24 aa fused to N- terminus of PA1029. Extension observed for 310/316 members of POG000991.
1215658	G → GG	PA1122	D3C65_20255	Reading frame is changed. Predicted product has 125 aa of PA1122 fused to 54aa instead of 22aa (PAO1). Similar change observed in 498/504 proteins of POG001082.
1275766	GA → G	PA1174	D3C65_19970	First 11 aa of PA1174 (napA) replaced by 16aa. Similar N-terminus is present in most proteins from POG001132.
2239555	A → AG	IG: PA2046-PA2047	D3C65_15395	Predicted product has PA2046 sequence extended for 316 aa (N – terminus). The sequence is similar to most of PA2046 orthologs (POG003399).
2355771	A → AG	PA2139	D3C65_14875	Reading frame is changed. Predicted product has 29 aa of PA2139 fused with 42aa instead of 11 aa (PAO1). Similar change in 6/12 members of POG008397.
2753522	G → GC	PA2451	D3C65_13240	PA2452 fused with PA2451. Similar fusion observed for most proteins from POG003088.
3016844	G → GC	PA2668	D3C65_12075	Reading frame and start codon changed leading to a product with last 56 aa identical to C-teminus of PA2668. Extended sequences in 295/301 orthologs from POG008397.
3083196	A → AG	PA2727	D3C65_11765	PA2727 fused with PA2728. Similar fusion observed for most proteins from POG002843.
3919508	G → GC	PA3503	D3C65_07595	Reading frame and start codon changed. Proposed product has the last 210aa identical with PA3503. Extended sequences in 69/73 orthologs from POG005142.
4539468	G → GC	PA4058	D3C65_04690	PA4059 fused with PA4060. Similar fusion observed for all proteins but PA4059/PA4060 from POG001625.
4888194	A → AG	PA4360	D3C65_23120	Removes start codon of PA4360. Proposed product has additional 122 aa fused to N- terminus of PA4360. This extension is observed for most members of POG003953.
5472415	C → CG	IG: PA4874-PA4875	D3C65_26560	Frameshift in sequence preceding PA4875. Predicted product is PA4875 extended for 81 aa. Longer sequence is typical for most orthologs from POG004503.

Table 3 SNPs and indels identified in *P. aeruginosa* PAO1161 genome resulting in amino acid changes relative to corresponding PAO1-UW proteins. Strain specific aa changes identified in PAO1161 are marked by bolded gene names.

Effect	PAO1-UW position	Nucleotide change	Amino acid change	PAO1 gene	Description
codon change and codon deletion	1102459	CGAGGCGGTGCTGGGCAGTGCCGAA → C	VLGSAEEAV513V	**PA1017 (*pauA*)**	pimeloyl-CoA synthetase
codon deletion	3436070	CGTGCATGGCACG → C	RAMH117	**PA3067**	transcriptional regulator
codon insertion	6176156	AGCTCGATCGCCTGCA→A	LDRLQ489	**PA5484 (*kinB*)**	histidine kinase
	5655229	G → GCGG	W226GW	PA5024	conserved hypothetical protein
start codon shift	1023047	GGCAAGAT → G	M1MVKGR	**PA0934 (*relA*)**	GTP pyrophosphokinase
missense	183697	T → G*	C310W	PA0159	probable transcriptional regulator
	504428	C → T	T103I	**PA0448 (*gcdR*)**	transcriptional regulator
	1589438	G → C#	G34A	PA1459	probable methyltransferase
	2669175	G → C#	P819A	PA2400 (*pvdJ*)	pyoverdine side chain peptide synthetase
	2806625	C → T	D249N	PA2491 (*mexS*)	probable oxidoreductase
	2807982	T → A*	F172I	PA2492 (*mexT*)	transcriptional regulator
	3132936	C → T	G108D	**PA2775 (*tsi4*)**	immunity protein
	3133912	C → T	S68F	**PA2776 (*pauB3*)**	FAD-dependent oxidoreductase
	3333256	G → A	V126M	**PA2976 (*rne*)**	ribonuclease E
	4212201	A → G*	H636R	PA3760	N-Acetyl-D-Glucosamine phosphotransferase transporter
	4251149	G → A	E108K	**PA3792 (*leuA*)**	2-isopropylmalate synthase
	4779026	T → A	H531L	**PA4270 (*rpoB*)**	DNA-directed RNA polymerase
	4869855	T → G	E158D	PA4341	probable transcriptional regulator

4924552	CG → GC*	PV177PL	PA4394	mechanosensitive ion channel protein
5336487	C → G	M405I	**PA4751 (*ftsH*)**	cell division protein
5743461	CG → GC*	T431S	PA5100 (*hutU*)	urocanase
5825480	G → A	A232T	**PA5173 (*arcC*)**	carbamate kinase
6115455	T → G[#]	K286N	PA5434 (*mtr*)	tryptophan permease
6131592	C → T	L169F	**PA5443 (*uvrD*)**	DNA helicase II
6174009	G → A	R221H	**PA5483 (*algB*)**	two-component response regulator
6233039	G → A	S162N	**PA5540**	hypothetical protein

* - observed in PAO1DSM / MPAO-1 (Klockgether et al., 2010)
[#] - observed in PAO1DSM / MPAO-1 and validated experimentally (Klockgether et al., 2010)

References

Aravind, L., Detlef D. Leipe, and Eugene V. Koonin. 1998. "Toprim—a Conserved Catalytic Domain in Type IA and II Topoisomerases, DnaG-Type Primases, OLD Family Nucleases and RecR Proteins." *Nucleic Acids Research* 26 (18): 4205–13. https://doi.org/10.1093/nar/26.18.4205.

Ball, Geneviève, Éric Durand, Andrée Lazdunski, and Alain Filloux. 2002. "A Novel Type II Secretion System in Pseudomonas Aeruginosa." *Molecular Microbiology* 43 (2): 475–85. https://doi.org/10.1046/j.1365-2958.2002.02759.x.

Ball, Geneviève, Véronique Viarre, Steven Garvis, Romé Voulhoux, and Alain Filloux. 2012. "Type II-Dependent Secretion of a Pseudomonas Aeruginosa DING Protein." *Research in Microbiology* 163 (6–7): 457–69. https://doi.org/10.1016/j.resmic.2012.07.007.

Bartosik, Aneta A., Krzysztof Glabski, Paulina Jecz, Sylwia Mikulska, Anna Fogtman, Marta Koblowska, and Grazyna Jagura-Burdzy. 2014. "Transcriptional Profiling of ParA and ParB Mutants in Actively Dividing Cells of an Opportunistic Human Pathogen Pseudomonas Aeruginosa." *PloS One* 9 (1): e87276. https://doi.org/10.1371/journal.pone.0087276.

Battle, Scott E., Folker Meyer, Jordi Rello, Vanderlene L. Kung, and Alan R. Hauser. 2008. "Hybrid Pathogenicity Island PAGI-5 Contributes to the Highly Virulent Phenotype of a Pseudomonas Aeruginosa Isolate in Mammals." *Journal of Bacteriology* 190 (21): 7130–40. https://doi.org/10.1128/JB.00785-08.

Bhowmik, Bijit K., April L. Clevenger, Hang Zhao, and Valentin V. Rybenkov. 2018. "Segregation but Not Replication of the Pseudomonas Aeruginosa Chromosome Terminates at Dif." *MBio* 9 (5). https://doi.org/10.1128/mBio.01088-18.

Campbell, E. A., N. Korzheva, A. Mustaev, K. Murakami, S. Nair, A. Goldfarb, and S. A. Darst. 2001. "Structural Mechanism for Rifampicin Inhibition of Bacterial Rna Polymerase." *Cell* 104 (6): 901–12.

Chand, Nikhilesh S., Anne E. Clatworthy, and Deborah T. Hung. 2012. "The Two-Component Sensor KinB Acts as a Phosphatase to Regulate Pseudomonas Aeruginosa Virulence." *Journal of Bacteriology* 194 (23): 6537–47. https://doi.org/10.1128/JB.01168-12.

Cianciotto, Nicholas P., and Richard C. White. 2017. "Expanding Role of Type II Secretion in Bacterial Pathogenesis and Beyond." *Infection and Immunity* 85 (5): e00014-17. https://doi.org/10.1128/IAI.00014-17.

Ciok, Anna, Karol Budzik, Marek K. Zdanowski, Jan Gawor, Jakub Grzesiak, Przemyslaw Decewicz, Robert Gromadka, Dariusz Bartosik, and Lukasz Dziewit. 2018. "Plasmids of Psychrotolerant Polaromonas Spp. Isolated From Arctic and Antarctic Glaciers – Diversity and Role in Adaptation to Polar Environments." *Frontiers in Microbiology* 9. https://doi.org/10.3389/fmicb.2018.01285.

Delavat, François, Ryo Miyazaki, Nicolas Carraro, Nicolas Pradervand, and Jan Roelof van der Meer. 2017. "The Hidden Life of Integrative and Conjugative Elements." *FEMS Microbiology Reviews* 41 (4): 512–37. https://doi.org/10.1093/femsre/fux008.

Doberenz, Sebastian, Denitsa Eckweiler, Olga Reichert, Vanessa Jensen, Boyke Bunk, Cathrin Spröer, Adrian Kordes, et al. 2017. "Identification of a Pseudomonas Aeruginosa PAO1 DNA Methyltransferase, Its Targets, and Physiological Roles." *MBio* 8 (1): e02312-16. https://doi.org/10.1128/mBio.02312-16.

Dunn, N. W., and B. W. Holloway. 1971. "Pleiotropy of P-Fluorophenylalanine-Resistant and Antibiotic Hypersensitive Mutants of Pseudomonas Aeruginosa." *Genetics Research* 18 (2): 185–97. https://doi.org/10.1017/S0016672300012593.

El-Sayed, A. K., J. Hothersall, and C. M. Thomas. 2001. "Quorum-Sensing-Dependent Regulation of Biosynthesis of the Polyketide Antibiotic Mupirocin in Pseudomonas Fluorescens NCIMB 10586." *Microbiology (Reading, England)* 147 (Pt 8): 2127–39. https://doi.org/10.1099/00221287-147-8-2127.

Fargier, Emilie, Micheál Mac Aogáin, Marlies J. Mooij, David F. Woods, John P. Morrissey, Alan D. W. Dobson, Claire Adams, and Fergal O'Gara. 2012. "MexT Functions as a Redox-Responsive Regulator Modulating Disulfide Stress Resistance in Pseudomonas Aeruginosa." *Journal of Bacteriology* 194 (13): 3502–11. https://doi.org/10.1128/JB.06632-11.

Finger, Judith, and Viji Krishnapillai. 1980. "Host Range, Entry Exclusion, and Incompatibility of Pseudomonas Aeruginosa FP Plasmids." *Plasmid* 3 (3): 332–42. https://doi.org/10.1016/0147-619X(80)90046-3.

Grindley, Nigel D. F., Katrine L. Whiteson, and Phoebe A. Rice. 2006. "Mechanisms of Site-Specific Recombination." *Annual Review of Biochemistry* 75: 567–605. https://doi.org/10.1146/annurev.biochem.73.011303.073908.

Hall, Alex R., James C. Iles, and R. Craig MacLean. 2011. "The Fitness Cost of Rifampicin Resistance in Pseudomonas Aeruginosa Depends on Demand for RNA Polymerase." *Genetics* 187 (3): 817–22. https://doi.org/10.1534/genetics.110.124628.

He, Jianxin, Regina L. Baldini, Eric Déziel, Maude Saucier, Qunhao Zhang, Nicole T. Liberati, Daniel Lee, Jonathan Urbach, Howard M. Goodman, and Laurence G. Rahme. 2004. "The Broad Host Range Pathogen Pseudomonas Aeruginosa Strain PA14 Carries Two Pathogenicity Islands Harboring Plant and Animal Virulence Genes." *Proceedings of the National Academy of Sciences of the United States of America* 101 (8): 2530–35.

Holloway, B. W. 1955. "Genetic Recombination in Pseudomonas Aeruginosa." *Journal of General Microbiology* 13 (3): 572–81. https://doi.org/10.1099/00221287-13-3-572.

Holloway, B. W., and B. Fargie. 1960. "Fertility Factors and Genetic Linkage in Pseudomonas Aeruginosa." *Journal of Bacteriology* 80 (September): 362–68.

Jatsenko, Tatjana, Andres Tover, Radi Tegova, and Maia Kivisaar. 2010. "Molecular Characterization of Rifr Mutations in Pseudomonas Aeruginosa and Pseudomonas Putida." *Mutation Research/Fundamental and Molecular Mechanisms of Mutagenesis* 683 (1): 106–14. https://doi.org/10.1016/j.mrfmmm.2009.10.015.

Johnson, Christopher M., and Alan D. Grossman. 2015. "Integrative and Conjugative Elements (ICEs): What They Do and How They Work." *Annual Review of Genetics* 49: 577–601. https://doi.org/10.1146/annurev-genet-112414-055018.

Kawalek, Adam, Aneta A. Bartosik, Krzysztof Glabski, and Grazyna Jagura-Burdzy. 2018. "Pseudomonas Aeruginosa Partitioning Protein ParB Acts as a Nucleoid-Associated Protein Binding to Multiple Copies of a ParS-Related Motif." *Nucleic Acids Research* 46 (9): 4592–4606. https://doi.org/10.1093/nar/gky257.

Kawalek, Adam, Krzysztof Glabski, Aneta Agnieszka Bartosik, Anna Fogtman, and Grazyna Jagura-Burdzy. 2017. "Increased ParB Level Affects Expression of Stress Response, Adaptation and Virulence Operons and Potentiates Repression of Promoters Adjacent to the High Affinity Binding Sites ParS3 and ParS4 in Pseudomonas Aeruginosa." *PLOS ONE* 12 (7): e0181726. https://doi.org/10.1371/journal.pone.0181726.

Khelik, Ksenia, Karin Lagesen, Geir Kjetil Sandve, Torbjørn Rognes, and Alexander Johan Nederbragt. 2017. "NucDiff: In-Depth Characterization and Annotation of Differences between Two Sets of DNA Sequences." *BMC Bioinformatics* 18 (1): 338. https://doi.org/10.1186/s12859-017-1748-z.

Klockgether, Jens, Antje Munder, Jens Neugebauer, Colin F. Davenport, Frauke Stanke, Karen D. Larbig, Stephan Heeb, et al. 2010. "Genome Diversity of Pseudomonas Aeruginosa PAO1 Laboratory Strains." *Journal of Bacteriology* 192 (4): 1113–21. https://doi.org/10.1128/JB.01515-09.

Klockgether, Jens, Oleg Reva, Karen Larbig, and Burkhard Tümmler. 2004. "Sequence Analysis of the Mobile Genome Island PKLC102 of Pseudomonas Aeruginosa C." *Journal of Bacteriology* 186 (2): 518–34.

Klockgether, Jens, and Burkhard Tümmler. 2017. "Recent Advances in Understanding Pseudomonas Aeruginosa as a Pathogen." *F1000Research* 6 (July). https://doi.org/10.12688/f1000research.10506.1.

Köhler, Thilo, Christian van Delden, Lasta Kocjancic Curty, Mehri Michea Hamzehpour, and Jean-Claude Pechere. 2001. “Overexpression of the MexEF-OprN Multidrug Efflux System Affects Cell-to-Cell Signaling in Pseudomonas Aeruginosa.” *Journal of Bacteriology* 183 (18): 5213–22. https://doi.org/10.1128/JB.183.18.5213-5222.2001.

Köhler, Thilo, Simone F. Epp, Lasta Kocjancic Curty, and Jean-Claude Pechère. 1999. “Characterization of MexT, the Regulator of the MexE-MexF-OprN Multidrug Efflux System of Pseudomonas Aeruginosa.” *Journal of Bacteriology* 181 (20): 6300–6305.

Komatsu, Tetsushi, Kazuhito Moriya, and Koki Horikoshi. 1994. “Preparation of Organic Solvent-Tolerant Mutants from Pseudomonas Aeruginosa Strain PAO1161.” *Bioscience, Biotechnology, and Biochemistry* 58 (9): 1754–55. https://doi.org/10.1271/bbb.58.1754.

Kujawa, Martyna, Maciej Lirski, Mateusz Ziecina, Joanna Drabinska, Marta Modzelan, and Elzbieta Kraszewska. 2017. “Nudix-Type RNA Pyrophosphohydrolase Provides Homeostasis of Virulence Factor Pyocyanin and Functions as a Global Regulator in Pseudomonas Aeruginosa.” *Molecular Microbiology* 106 (3): 381–94. https://doi.org/10.1111/mmi.13771.

Kung, A. H. C., and B. T. O. Lee. 1975. “Genetic Analysis of Radiation Sensitive and Chemical-Mutagen Sensitive Mutants of Pseudomonas Aeruginosa.” *Mutation Research/Fundamental and Molecular Mechanisms of Mutagenesis* 27 (2): 191–99. https://doi.org/10.1016/0027-5107(75)90078-0.

Lamarche, Martin G., and Eric Déziel. 2011. “MexEF-OprN Efflux Pump Exports the Pseudomonas Quinolone Signal (PQS) Precursor HHQ (4-Hydroxy-2-Heptylquinoline).” *PLOS ONE* 6 (9): e24310. https://doi.org/10.1371/journal.pone.0024310.

Lasocki, Krzysztof, Aneta A. Bartosik, Jolanta Mierzejewska, Christopher M. Thomas, and Grazyna Jagura-Burdzy. 2007. “Deletion of the ParA (Soj) Homologue in Pseudomonas Aeruginosa Causes ParB Instability and Affects Growth Rate, Chromosome Segregation, and Motility.” *Journal of Bacteriology* 189 (15): 5762–72. https://doi.org/10.1128/JB.00371-07.

Laudy, Agnieszka E., Paula Osińska, Alicja Namysłowska, Olga Zając, and Stefan Tyski. 2015. “Modification of the Susceptibility of Gram-Negative Rods Producing ESβLS to β-Lactams by the Efflux Phenomenon.” *PLOS ONE* 10 (3): e0119997. https://doi.org/10.1371/journal.pone.0119997.

Liu, Meng, Xiaobin Li, Yingzhou Xie, Dexi Bi, Jingyong Sun, Jun Li, Cui Tai, Zixin Deng, and Hong-Yu Ou. n.d. “ICEberg 2.0: An Updated Database of Bacterial Integrative and Conjugative Elements.” *Nucleic Acids Research*. Accessed November 19, 2018. https://doi.org/10.1093/nar/gky1123.

Luong, Preston M., Benjamin D. Shogan, Alexander Zaborin, Natalia Belogortseva, Joshua D. Shrout, Olga Zaborina, and John C. Alverdy. 2014. “Emergence of the P2 Phenotype in Pseudomonas Aeruginosa PAO1 Strains Involves Various Mutations in MexT or MexF.” *Journal of Bacteriology* 196 (2): 504–13. https://doi.org/10.1128/JB.01050-13.

Manavathi, Bramanandam, Suresh B. Pakala, Purushotham Gorla, Mike Merrick, and Dayananda Siddavattam. 2005. “Influence of Zinc and Cobalt on Expression and Activity of Parathion Hydrolase from Flavobacterium Sp. ATCC27551.” *Pesticide Biochemistry and Physiology* 83 (1): 37–45. https://doi.org/10.1016/j.pestbp.2005.03.007.

Maseda, Hideaki, Kohjiro Saito, Akira Nakajima, and Taiji Nakae. 2000. “Variation of the MexT Gene, a Regulator of the MexEF-OprN Efflux Pump Expression in Wild-Type Strains of Pseudomonas Aeruginosa.” *FEMS Microbiology Letters* 192 (1): 107–12. https://doi.org/10.1016/S0378-1097(00)00419-5.

Mathee, Kalai, Giri Narasimhan, Camilo Valdes, Xiaoyun Qiu, Jody M. Matewish, Michael Koehrsen, Antonis Rokas, et al. 2008. “Dynamics of Pseudomonas Aeruginosa Genome Evolution.” *Proceedings of the National Academy of Sciences of the United States of America* 105 (8): 3100–3105. https://doi.org/10.1073/pnas.0711982105.

Mavrodi, Dmitri V., Joyce E. Loper, Ian T. Paulsen, and Linda S. Thomashow. 2009. “Mobile Genetic Elements in the Genome of the Beneficial Rhizobacterium Pseudomonas

Fluorescens Pf-5.” *BMC Microbiology* 9 (January): 8. https://doi.org/10.1186/1471-2180-9-8.

Papagiannitsis, C. C., V. Studentova, F. Ruzicka, R. Tejkalova, and J. Hrabak. 2013. “Molecular Characterization of Metallo-β-Lactamase-Producing Pseudomonas Aeruginosa in a Czech Hospital (2009-2011).” *Journal of Medical Microbiology* 62 (Pt 6): 945–47. https://doi.org/10.1099/jmm.0.056119-0.

Qiu, Xiaoyun, Aditi U. Gurkar, and Stephen Lory. 2006. “Interstrain Transfer of the Large Pathogenicity Island (PAPI-1) of Pseudomonas Aeruginosa.” *Proceedings of the National Academy of Sciences of the United States of America* 103 (52): 19830–35. https://doi.org/10.1073/pnas.0606810104.

Rolfe, B., and B. W. Holloway. 1968. “Genetic Control of DNA Specificity in Pseudomonas Aeruginosa.” *Genetics Research* 12 (1): 99–102. https://doi.org/10.1017/S0016672300011678.

Romaniuk, Krzysztof, Tomasz Krucon, Przemyslaw Decewicz, Adrian Gorecki, and Lukasz Dziewit. 2017. “Molecular Characterization of the PA3J1 Plasmid from the Psychrotolerant Antarctic Bacterium Pseudomonas Sp. ANT_J3.” *Plasmid* 92 (July): 49–56. https://doi.org/10.1016/j.plasmid.2017.08.001.

Ryan Withers, T., F. Heath Damron, Yeshi Yin, and Hongwei D. Yu. 2013. “Truncation of Type IV Pilin Induces Mucoidy in Pseudomonas Aeruginosa Strain PAO579.” *MicrobiologyOpen* 2 (3): 459–70. https://doi.org/10.1002/mbo3.86.

Severinov, K., M. Soushko, A. Goldfarb, and V. Nikiforov. 1993. “Rifampicin Region Revisited. New Rifampicin-Resistant and Streptolydigin-Resistant Mutants in the Beta Subunit of Escherichia Coli RNA Polymerase.” *The Journal of Biological Chemistry* 268 (20): 14820–25.

Shintani, Masaki, Zoe K. Sanchez, and Kazuhide Kimbara. 2015. “Genomics of Microbial Plasmids: Classification and Identification Based on Replication and Transfer Systems and Host Taxonomy.” *Frontiers in Microbiology* 6. https://doi.org/10.3389/fmicb.2015.00242.

Sidorenko, Julia, Tatjana Jatsenko, and Maia Kivisaar. 2017. “Ongoing Evolution of Pseudomonas Aeruginosa PAO1 Sublines Complicates Studies of DNA Damage Repair and Tolerance.” *Mutation Research/Fundamental and Molecular Mechanisms of Mutagenesis* 797–799 (March): 26–37. https://doi.org/10.1016/j.mrfmmm.2017.03.005.

Sobel, Mara L., Shadi Neshat, and Keith Poole. 2005. “Mutations in PA2491 (MexS) Promote MexT-Dependent MexEF-OprN Expression and Multidrug Resistance in a Clinical Strain of Pseudomonas Aeruginosa.” *Journal of Bacteriology* 187 (4): 1246–53. https://doi.org/10.1128/JB.187.4.1246-1253.2005.

Stanisich, Vilma, and B. W. Holloway. 1969a. “Conjugation in PSEUDOMONAS AERUGINOSA.” *Genetics* 61 (2): 327–39.

———. 1969b. “Genetic Effects of Acridines on Pseudomonas Aeruginosa.” *Genetics Research* 13 (1): 57–70. https://doi.org/10.1017/S0016672300002731.

Stover, C. K., X. Q. Pham, A. L. Erwin, S. D. Mizoguchi, P. Warrener, M. J. Hickey, F. S. Brinkman, et al. 2000. “Complete Genome Sequence of Pseudomonas Aeruginosa PAO1, an Opportunistic Pathogen.” *Nature* 406 (6799): 959–64. https://doi.org/10.1038/35023079.

Uwate, Maki, Yu-ki Ichise, Akihiro Shirai, Takeshi Omasa, Taiji Nakae, and Hideaki Maseda. 2013. “Two Routes of MexS-MexT-Mediated Regulation of MexEF-OprN and MexAB-OprM Efflux Pump Expression in Pseudomonas Aeruginosa.” *Microbiology and Immunology* 57 (4): 263–72. https://doi.org/10.1111/1348-0421.12032.

Winsor, Geoffrey L., Emma J. Griffiths, Raymond Lo, Bhavjinder K. Dhillon, Julie A. Shay, and Fiona S. L. Brinkman. 2016. “Enhanced Annotations and Features for Comparing Thousands of Pseudomonas Genomes in the Pseudomonas Genome Database.” *Nucleic Acids Research* 44 (D1): D646–53. https://doi.org/10.1093/nar/gkv1227.

Wozniak, Rachel A. F., and Matthew K. Waldor. 2010. “Integrative and Conjugative Elements: Mosaic Mobile Genetic Elements Enabling Dynamic Lateral Gene Flow.” *Nature Reviews Microbiology* 8 (8): 552–63. https://doi.org/10.1038/nrmicro2382.

Yin, Yeshi, T. Ryan Withers, John R. W. Govan, Shannon L. Johnson, and Hongwei D. Yu. 2013. “Draft Genome Sequence of a Stable Mucoid Strain of Pseudomonas Aeruginosa PAO581 with a MucA25 Mutation.” *Genome Announcements* 1 (5). https://doi.org/10.1128/genomeA.00834-13.